Detection of synchronized oscillations in the electroencephalogram: An evaluation of methods

NICK YEUNG,[1] RAFAL BOGACZ,[2] CLAY B. HOLROYD,[1] AND JONATHAN D. COHEN[1,3]

[1]Department of Psychology, Princeton University, Princeton, New Jersey, USA
[2]Department of Applied and Computational Mathematics, Princeton University, Princeton, New Jersey, USA
[3]Department of Psychiatry, University of Pittsburgh, Pittsburgh, Pennsylvania, USA

Abstract

The signal averaging approach typically used in ERP research assumes that peaks in ERP waveforms reflect neural activity that is uncorrelated with activity in the ongoing EEG. However, this assumption has been challenged by research suggesting that ERP peaks reflect event-related synchronization of ongoing EEG oscillations. In this study, we investigated the validity of a set of methods that have been used to demonstrate that particular ERP peaks result from synchronized EEG oscillations. We simulated epochs of EEG data by superimposing phasic peaks on noise characterized by the power spectrum of the EEG. When applied to the simulated data, the methods in question produced results that have previously been interpreted as evidence of synchronized oscillations, even though no such synchrony was present. These findings suggest that proposed analysis methods may not effectively disambiguate competing views of ERP generation.

Descriptors: Electroencephalography, Event-related potential, Synchrony, Oscillations, Phase resetting

A common approach to the study of electroencephalographic (EEG) activity is to assess voltage changes that are time-locked to events of interest such as stimuli or responses. When one calculates the average voltage across a number of EEG epochs that are each time-locked to a repetition of an event of interest, characteristic waveforms are observed. The event-related brain potentials (ERPs) thus revealed consist of a series of positive and negative peaks occurring at a fixed time relative to the event. These component peaks are considered to reflect phasic activity in one or more discrete brain areas, and are studied with the assumption that they index meaningful aspects of cognitive processing (see, e.g., Coles, Gratton, & Fabiani, 1990; Coles & Rugg, 1995).

An issue of current debate is the relation between ERPs and rhythmic activity in the ongoing EEG. Through Fourier and wavelet analyses, it has been shown that rhythmic activity within specific frequency bands—delta (0.5–4 Hz), theta (4–8 Hz), alpha (8–12 Hz), beta (12–20 Hz), and gamma (20–70 Hz)—appears to index meaningful cognitive processes (e.g., Kahana, Sekuler, Caplan, Kirschen, & Madsen, 1999; Klimesch, 1999; Tallon-Baudry & Bertrand, 1999). The signal averaging approach typically used in ERP research treats this oscillatory EEG activity as background "noise" in which the ERP "signal" is embedded. According to this *classical view*, ERPs reflect phasic bursts of activity in one or more discrete brain regions that occur time-locked to particular events of interest, whereas the background EEG comprises activity that is uncorrelated with these events—a mixture of ongoing rhythmic activity that reflects the overall state of the processing network (e.g., Gevins, Smith, McEvoy, & Yu, 1997; Pfurtscheller & Lopes da Silva, 1999) and ERPs evoked by nonexperimental events. At various times over the last 30 years, however, the classical view has been challenged by the proposal that ERPs should not be regarded as uncorrelated with the background EEG, but are instead generated by event-related reorganization of this ongoing rhythmic activity (Başar, 1980; Karakaş, Erzengin, & Başar, 2000; Luu & Tucker, 2001; Makeig, Westerfield, et al., 2002; Sayers, Beagley, & Henshall, 1974). The present research aims to evaluate one set of analysis methods that have been used to support this synchronized oscillation hypothesis.

Phasic Events and Synchronized Oscillations

The competing views of ERP generation are illustrated in Figure 1. The left panel illustrates the classical view, in which phasic event-related activity—the period of which is indicated by the shaded region—is embedded in ongoing fluctuations that are inconsistent across trials. For illustrative purposes, the figure shows a situation in which a burst of phasic activity is visible in individual EEG epochs. In some situations, however, phasic activity may not be clearly evident in individual EEG epochs because it is small relative to the amplitude of fluctuations in the background EEG. Nonetheless, when a number of EEG epochs are averaged together, task-irrelevant fluctuations in the ongoing EEG cancel out so that the resulting ERP waveforms reflect only phasic activity that is consistent across trials. This signal averaging approach, grounded in the study of intracranial recordings of evoked neural activity (e.g., Domino, Matsuoka, Waltz, & Cooper, 1964; Goff, Allison, & Vaughan, 1978; Shah et al., 2004), has formed the basis for several decades of ERP research that has been very successful in identifying ERP components corresponding to a wide range of cognitive processes (e.g., Coles et al., 1990; Coles & Rugg, 1995; Goff et al., 1978; Vaughan, 1969).

Although the signal averaging approach has formed the foundation of a successful ERP research program, it has not gone unchallenged. It has often been noted that signal averaging may result in the loss of critical information about intertrial variability in neural activity—because, by definition, averaging emphasizes activity that is consistent across trials (Vaughan, 1969; Weinberg, 1978). This criticism has most often been expressed in the context of the hypothesis, first proposed by Sayers et al. (1974), that ERPs may be generated by reorganization of ongoing rhythmic activity in the EEG, rather than being uncorrelated with this activity. This hypothesis challenges the assumption of the classical view that peaks apparent in ERPs reflect phasic, event-related bursts of neural activity that are unrelated to the background EEG: Instead, ERP peaks may be generated by event-related synchronization of oscillatory activity in the EEG that occurs with little or no accompanying change in the magnitude of those oscillations.
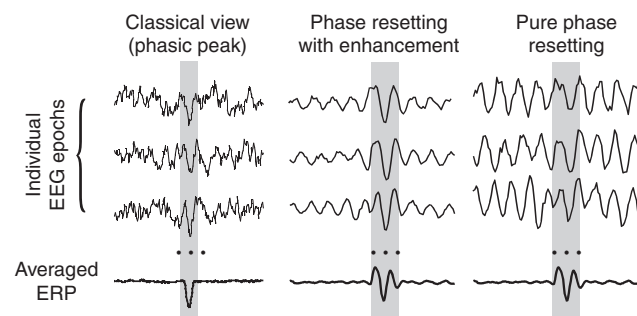

Figure 1. Comparison of the classical and synchronized oscillation theories of the origin of ERPs. Each panel shows examples of idealized EEG epochs, each corresponding to a single trial, along with the ERP (bottom line) calculated as the average of many such epochs. The left panel shows the classical view, in which ERP components are held to reflect phasic neural events that are embedded in background EEG noise. The center and right panels illustrate how synchronization of EEG oscillations may also contribute to the ERP, either by pure phase resetting (right panel) or by phase resetting and enhancement (i.e., increases in amplitude) of oscillations (center panel).

We distinguish two variants of the synchronized oscillation hypothesis. The right-hand panel of Figure 1 illustrates the case of *pure phase resetting*, which has been proposed as an account of the N1 peaks evoked by auditory (Jansen, Agarwal, Hegde, & Boutos, 2003; Sayers et al., 1974) and visual (Klimesch et al., 2004; Makeig, Westerfield, et al., 2002) stimuli. In this case, the occurrence of an event leads to resetting of the phase of ongoing rhythmic activity but does not cause any change in the overall magnitude of voltage fluctuations in the EEG (i.e., there is phase modulation but no amplitude modulation of the EEG; Penny, Kiebel, Kilner, & Rugg, 2002). As a consequence of phase resetting, there is a period during which there is consistency (or *coherence*) of EEG phase across trials. This phase coherence is apparent visually in Figure 1 (right panel) as the alignment of peaks and troughs in EEG traces from individual trials during the period indicated by the shaded region. The net result is that the averaged ERP is characterized by a phasic burst of activity around the time of the event—caused by phase-resetting of rhythmic EEG activity and consequent increase in coherence during that epoch—and is relatively flat during periods in which there is no phase coherence across trials.

The center panel of Figure 1 illustrates the case of *phase resetting with enhancement*, in which there is an event-related increase in the amplitude of the oscillation in addition to phase resetting. In this case, the transient signal apparent in the averaged ERP in the period just after the event may also be apparent to some degree on individual trials. Phase resetting with enhancement has been proposed as an explanation for many ERP peaks, including the N1, N2, and P3 (Başar, 1980; Başar, Başar-Eroglu, Parnefjord, Rahn, & Schürmann, 1992; Karakaş et al., 2000). More recently, it has been suggested that the error-related negativity (Ne or ERN)—an ERP component seen following errors in choice RT tasks (Falkenstein, Hohnsbein, Hoorman, & Blanke, 1990; Gehring, Goss, Coles, Meyer, & Donchin, 1993)—may be generated by phase resetting and enhancement of theta frequency oscillations in medial frontal cortex (Luu & Tucker, 2001).

Methods for Detecting Synchronized Oscillations

Various methods have been proposed to provide evidence of synchronized oscillations. Pure phase resetting can be demonstrated by showing that particular ERP peaks are generated by event-related changes in the phase distribution of the EEG, without corresponding increases in spectral power at frequencies present in the ERP peak. Such demonstrations have been made for some early auditory (Jansen et al., 1993; Sayers et al., 1974) and visual (Klimesch et al., 2004; Makeig, Westerfield, et al., 2002) evoked potentials, as well as for theta oscillations associated with working memory processes (Rizzuto et al., 2003). Pure phase resetting is likewise easily ruled out by showing that ERPs are associated with increases in spectral power (Jervis, Nichols, Johnson, Allen, & Hudson, 1983; Shah et al., 2004).

It is more difficult to distinguish between the classical view and the phase resetting with enhancement hypothesis, both of which predict that ERP peaks are associated with increased power in some frequency range. Such power increases are observed for the N2, P3, and Ne/ERN (e.g., Demiralp, Ademoglu, Schürmann, Başar-Eroglu, & Başar, 1999; Karakaş et al., 2000, Makeig, Luu, & Tucker, 2002). In such cases, further analysis methods are required to distinguish between the competing accounts. To this end, a number of methods have recently been used to provide evidence that ERP peaks result from modulations of

the rhythmic EEG rather than phasic events (e.g., Luu & Tucker, 2001; Makeig, Westerfield, et al., 2002). These analyses suggest that certain diagnostic properties are expected if ERPs reflect synchronized oscillations. Among these properties are the following.

1. *Uneven phase distributions and increased intertrial coherence associated with the ERP peak.* The most direct prediction of the synchronized oscillation hypothesis is that there should be an uneven distribution of the phase of oscillations across trials in the period following the event of interest. Phase information from Fourier or wavelet analyses can be used in two ways to assess phase synchronization (e.g., Makeig, Westerfield, et al., 2002). A first, qualitative approach is to plot the EEG data after sorting them according to their spectral phase at a particular frequency, so that visual inspection can be used to determine whether ERP components coincide with periods in which EEG activity at that frequency tends to be in phase across trials. A second, more quantitative approach is to measure the correlation across trials in the EEG spectral phase for particular frequency ranges. The presence of this *intertrial phase coherence* (also called *phase-locking factor* [Tallon-Baudry, Bertrand, Delpuech, & Pernier, 1996] and *phase-locking index* [Klimesch et al., 2004]) is considered evidence for the hypothesis that an ERP peak is generated by phase resetting of EEG oscillations (e.g., Makeig, Westerfield, et al., 2002).

2. *Appearance of oscillations in bandpass filtered ERP data.* As is evident in Figure 1, synchronization of oscillations should produce a series of peaks of diminishing amplitude, *ringing* that should be apparent for as long as the oscillations remain partially in phase across epochs. However, the absence of such ringing is not conclusive evidence of the absence of synchronized oscillations: It could be that ringing is present but is masked by subsequent ERP peaks. One suggestion is that bandpass filtering around the peak frequency of the component of interest can be used to remove the contribution of other superimposed components, thus uncovering the underlying oscillations (e.g., Luu & Tucker, 2001).

3. *Correlation between ERP amplitude and spectral power in the EEG.* If ERPs are produced by synchronization of ongoing oscillations in the EEG, then the amplitude of the ERPs should depend upon the amplitude of these oscillations. Thus, amplitude sorting is another method that has been used to provide evidence of synchronized oscillations (e.g., Makeig, Westerfield, et al., 2002). This method involves selecting subsets of data comprising trials with the highest and lowest EEG power at the peak frequency of the component of interest. The predicted result is that the ERP should have a high amplitude in the subset of trials with the highest EEG power, and should be small or absent in trials with lowest EEG power. This finding has previously been reported for visual N1 data sorted according to alpha power (Makeig, Westerfield, et al., 2002).

4. *Shared scalp distribution of spectral power in the ERP and EEG.* Along similar lines, if ERPs are produced by synchronization of ongoing oscillations in the EEG, one might expect that the scalp distribution of spectral power in the ERP should mirror the scalp distribution of spectral power in the EEG. This relationship between EEG and ERP power has been observed for poststimulus theta and alpha power that contributes to the N1 evoked by visual stimuli (e.g., Makeig, Westerfield, et al., 2002).

5. *Greater spectral power in the ERP than expected by chance.* According to the classical view, the contribution of EEG noise to the averaged ERP should tend toward zero as more epochs are averaged together, a fact that underpins the typical signal averaging approach. In fact, the expected strength of the contribution of EEG noise to the averaged ERP is easily calculated as S_{EEG}/N, where S_{EEG} is the power in the single-trial EEG at a given frequency and N is the number of EEG epochs. Power at that frequency will only equal this expected value if the phase of this frequency component of the EEG is randomly distributed across trials. Hence, to the extent that there is more power than expected in the averaged ERP, one can infer that the phase distribution of the EEG is not random. Observations of this kind of phase coherence have been interpreted as evidence for the phase resetting account (e.g., Makeig, Westerfield, et al., 2002).

Research Overview

In the present research, we evaluate the five analysis methods described above, each of which identifies a property of empirical EEG data that has been taken to indicate the presence of synchronized oscillations. These methods make the critical assumption that the observed properties should not be apparent if the classical view of ERP generation is correct (i.e., if the ERP reflects the addition of phasic peaks to uncorrelated background noise). However, the validity of this assumption has not yet been tested; that is, it has not yet been tested whether the proposed analysis methods can provide clear evidence against the classical view.

To address this issue, we generated simulated EEG data according to the classical view, comprising phasic peaks embedded in background noise. We then applied each analysis method to both the simulated data and to empirically derived data. Of interest was whether the methods would produce results that suggest the presence of synchronized oscillations when applied to our simulated data (in which there was no phase resetting). If so, then the ability of these methods to distinguish between phasic events and oscillatory activity must be called into question. As an illustrative example, the tested data involved the Ne/ERN. Our aim is not to determine whether the Ne/ERN reflects phasic neural activity or phase resetting of EEG oscillations. Rather, our aim is to investigate whether the methods can provide unambiguous evidence of synchronized oscillations in this example data set.

Methods

Experimental Details

The empirical data are taken from an existing study (Yeung, Botvinick, & Cohen, in press) in which the full experimental details are presented. Briefly, 16 participants each performed 816 trials of a speeded choice RT task (Eriksen & Eriksen, 1974). While they performed the task, the EEG was recorded using Ag/AgCl electrodes placed in an extended 10–20 system montage in a fabric cap (Neurosoft, Inc.), referenced to linked mastoids. The signals were digitized at 250 Hz. Response-locked epochs, from 400 ms before the response until 400 ms after, were extracted offline from the EEG separately for correct and incorrect responses. We are concerned with the ERPs observed following incorrect responses. There were 973 error-trial epochs in the data for all 16 participants, and these are the data presented, taken from 31

electrode positions: FP1, FP2, AFz, F7, F3, Fz, F4, F8, FT7, FC3, FCz, FC4, FT8, T7, C3, Cz, C4, T8, TP7, CP3, CPz, CP4, TP8, P7, P3, Pz, P4, P8, O1, Oz, O2. Our analysis of scalp topography uses all 31 electrodes; other analyses focus on electrode location FCz, at which the Ne/ERN is maximal.

Simulation Details

We simulated 973 epochs of EEG data, sampled at 250 Hz and running from -400 ms to 400 ms so as to match the empirical data. The epochs were constructed by adding two phasic ERP peaks onto uncorrelated background noise. Figure 2a illustrates the two phasic peaks used. The first, corresponding to the Ne/ERN, consisted of a negative-going, half-cycle of a 5-Hz sinusoid, the latency of which varied across epochs ($M = 60$ ms; $SD = 32$ ms). Peak amplitude was constant across trials, but varied across simulated scalp locations to mimic the frontocentral distribution of the Ne/ERN. For simplicity, we chose to simulate the scalp topography of the Ne/ERN peak with a single dipole model, with location: $x = 0$ cm (midline), $y = 2.5$ cm (anterior to T7–T8 axis), $z = 6.5$ cm (superior to FPz–Oz axis); and orientation: $x = 0$, $y = 0.1$, $z = 0.99$. Scalp voltage distributions for dipole models were derived using a standard forward model algorithm (BESA 2000; www.besa.de). At its FCz maximum, the base-to-peak amplitude of the simulated Ne/ERN was 25 μV. With latency jitter, the amplitude of the negative peak in the averaged ERP was roughly 16 μV, matching the empirically observed Ne/ERN peak. The second component, corresponding to the Pe (described below), consisted of an unjittered slow wave of frequency 1 Hz, with a positive peak at time 200 ms. Again, the scalp topography of the component was simulated with a single dipole model (location: $x = 0$, $y = 0.5$, $z = 0.45$; orientation: $x = 0$, $y = -0.25$, $z = 0.97$). At its maximum at simulated electrode location Cz, the base-to-peak amplitude of the slow-wave component was 22 μV. Figure 2b shows that the summation of these two components (black line) results in an ERP waveform that closely mimics the morphology of the empirically observed ERP (gray line).

The two phasic peaks were added to uncorrelated background EEG "noise" that was simulated by summing together 50 sinusoids of randomly varying frequency and phase (with different random values of phase and frequency generated for each simulated epoch). The frequencies were chosen to span the range from 0.1 to 125 Hz, the phases varied randomly between 0 and 2π. The maximum amplitude of any single frequency component of the background EEG (at 0.1 Hz) was set to be 20 μV. Within this constraint, the amplitude of the sinusoid at each frequency was scaled to match the power spectrum of the EEG (estimated from nonerror trial empirical data).[1] Because this process amounts to an inverse-Fourier transform (with randomized phase) of a spectral analysis of real data, the simulated data match closely the surface features of empirically observed EEG data (as described below). Although the frequency characteristics of the EEG are known to vary across electrode locations, we used the same frequency spectrum to simulate the EEG for all electrode locations. This simplifying assumption allowed us to evaluate directly the extent to which the spectral characteristics of the EEG will be influenced by the addition of phasic ERP peaks with

Figure 2. Construction of the simulated ERP. a: The simulated ERP components, corresponding to the Ne/ERN (upper line) with a frontocentral distribution, and the Pe (lower line) with a diffuse posterior distribution. b: Response-locked averaged ERP at FCz, separately for simulated data with no background EEG noise (black line) and for empirical data (gray line).

a particular frequency spectrum and scalp topography, an issue addressed in Analyses 4 and 5.

The simulation parameters described above were chosen to fit the observed empirical data. As detailed below, the simulated data, though very simple in structure, accurately replicate the primary features of the empirical data. Nonetheless, to reiterate, our aim here is not to promote this simple model as the "true" account of the Ne/ERN. Rather, we simply wanted to evaluate whether properties that have been proposed to provide evidence of synchronized oscillations could be observed in the absence of such activity.

Results

Basic Features

Empirical data. The principal features of the empirical data are shown in Figure 3. Figure 3a plots eight example EEG epochs from electrode FCz (black lines), together with corresponding 4–12 Hz filtered waveforms (gray lines).[2] A negative peak corresponding to the Ne/ERN can be observed just after the response in some of the individual epochs, but this peak is not markedly greater in amplitude than theta activity observed pre- and post-response in the individual EEG epochs (gray lines). However, ongoing theta activity does not occur phase-locked to the response, and hence averages out to roughly zero across trials. As a

---

[1]We also ran simulations using white noise and 1/f noise. The results were not materially different from those presented. The critical feature of the noise is that it must have appreciable energy in the frequency range of the phasic peak, as will become apparent.
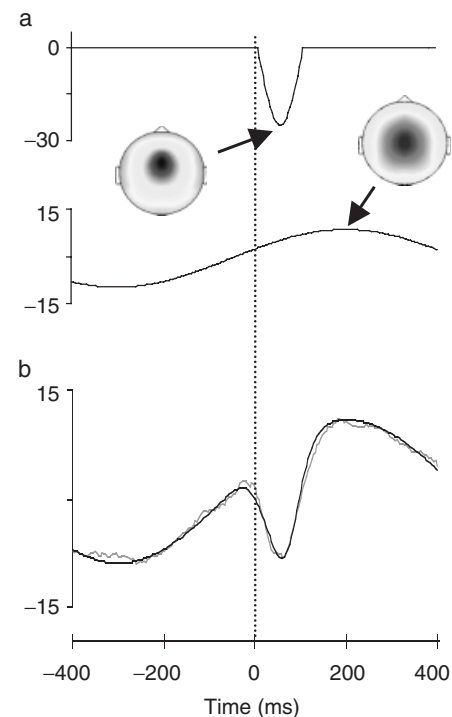
[2]All digital filtering reported here used a finite impulse response filter with zero phase-shift, as has been used in previous research (e.g., Luu & Tucker, 2001).
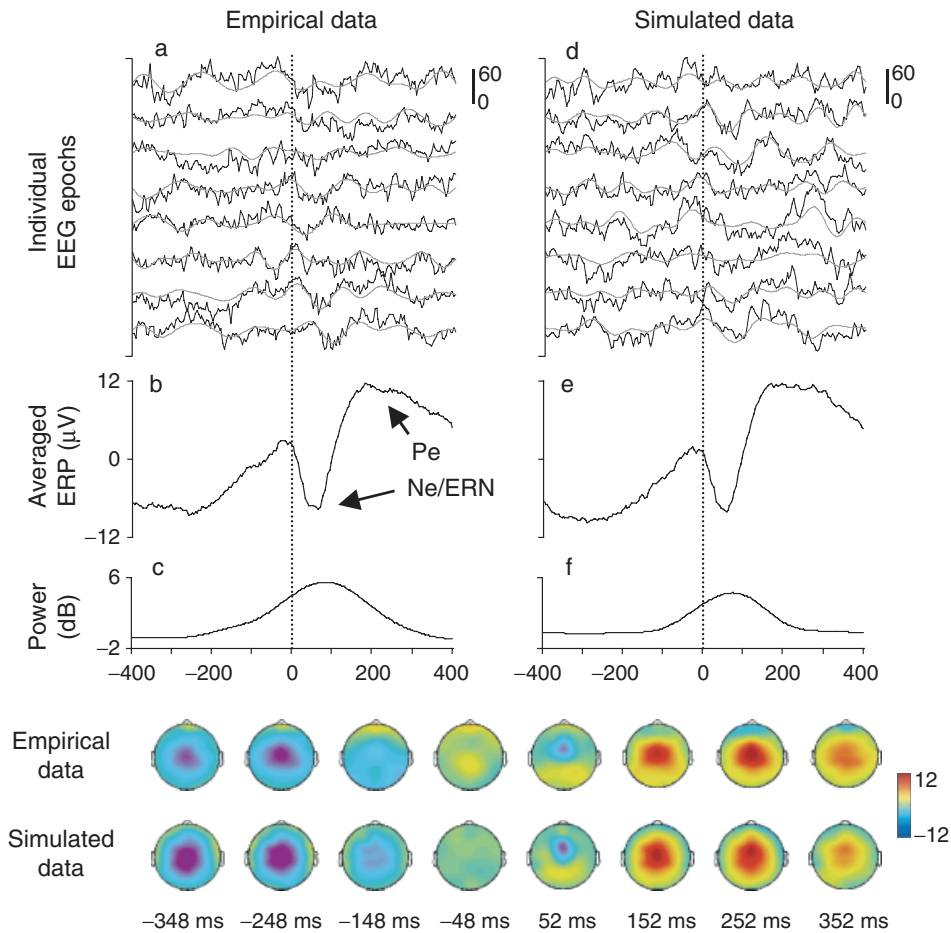
Figure 3. Comparison of surface features of empirical and simulated data. a: Examples of eight empirical EEG epochs (black lines) and 4–12 Hz filtered waveforms (gray lines), taken from electrode FCz. b: Response-locked averaged ERP for the empirical data at electrode location FCz. c: Relative 6-Hz EEG power at FCz across the epoch of the empirical data. d–f: Corresponding analyses of the simulated data. Note that different vertical scales are used for the EEG and ERP data, and that 0 ms is the time of the response to which the data are aligned. Lower panel: Scalp topography of empirical and simulated data between − 348 ms and +352 ms.

consequence, the Ne/ERN is clearly evident in the averaged ERP (Figure 3b) as a sharp negative deflection peaking about 60 ms after the response. Prior to the Ne/ERN, the ERP waveform is negative, becoming increasingly positive. The Ne/ERN is followed by a slow-wave positivity that has been labeled the error positivity (Pe; Falkenstein et al., 1995). Figure 3c shows that EEG theta power is markedly increased at the time of the Ne/ERN. The lower panel of Figure 3 illustrates the scalp topography of the peaks in the ERP waveform: The Ne/ERN is evident as a localized frontocentral negativity peaking ∼52 ms postresponse, whereas the slow-wave component has a broader, more posterior focus, peaking ∼200 ms after the response.

Simulated data. Corresponding analyses of the simulated data are presented in Figure 3d–f. The simulated data accurately replicate the surface features of the empirical data described above. Figure 3d shows eight example simulated EEG epochs (black lines) and corresponding 4–12 Hz filtered waveforms (gray lines). As was the case for the empirical data, an Ne/ERN peak is somewhat evident in single-trial EEG traces as part of ongoing theta activity, but theta activity is also observed pre- and postresponse. However, theta activity in the background EEG occurs with random phase and therefore cancels out in the av-

eraged ERP (Figure 3e) to reveal a clear negative peak corresponding to the Ne/ERN. Figure 3f shows that theta power in the simulated EEG is substantially increased by the addition of the phasic Ne/ERN peak. The lower panel of Figure 3 illustrates that our simulated data also capture well the scalp topography evident in the empirical data, with a frontocentral Ne/ERN peak at ∼52 ms that is superimposed on a slow positive-going wave with a more posterior scalp topography, peaking at ∼200 ms.

Analysis 1: Phase Distribution and Intertrial Coherence

Figure 4a presents single-trial data for the 973 empirical EEG epochs. Each epoch is plotted as a horizontal line with voltage coded by color: negative voltages in blue and positive voltages in red. The data are sorted from top to bottom according to the relative phase of 6-Hz activity in the period from 180 ms before the response until 320 ms after.[3] Because the Ne/ERN is strongest in the theta frequency band, sorting by the phase of 6-Hz activity essentially sorts the trials by Ne/ERN latency. The figure shows that there is variability in theta phase across trials, but that some latencies are more common than others. Specifically, a

---

[3]The calculation of EEG phase was performed using a three-cycle Hanning-windowed sinusoidal wavelet.
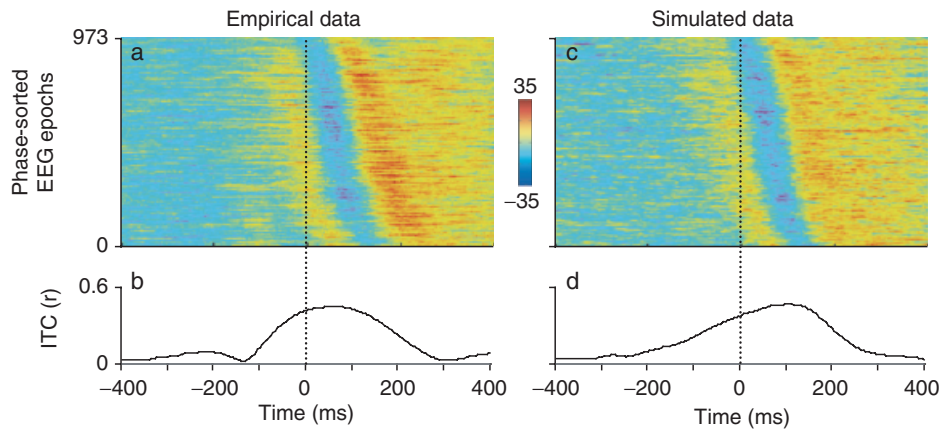
Figure 4. Analysis of phase coherence. a: Single-trial empirical EEG epochs from electrode FCz sorted according to phase at the theta frequency. b: Intertrial phase coherence (ITC) of 6-Hz activity in empirical EEG data at FCz. c,d: Corresponding analyses of simulated data.

negative peak with theta power, the Ne/ERN, occurs 20–80 ms after the response on most trials. As a consequence, the phase of theta activity is unevenly distributed across trials: There is *phase coherence*. This notion is confirmed by a quantitative analysis of the intertrial coherence (ITC) of 6-Hz activity (Figure 4b). As described above, intertrial coherence provides a measure of the consistency in relative phase across trials. Figure 4b shows that there is a marked increase in intertrial phase coherence of 6-Hz activity at the time of the Ne/ERN.

Thus, the empirical data are characterized by the presence of an uneven phase distribution and a marked increase in intertrial phase coherence during the time of the Ne/ERN. However, as shown in the right-hand panel of Figure 4, the simulated data demonstrate corresponding properties even though they contain no synchronized oscillations. Figure 4c plots phase-sorted single-trial EEG epochs, which show a weighting toward a dominant phase with a negative peak occurring 20–80 ms after the response, resulting in a marked increase in intertrial phase coherence of 6-Hz activity at this time (Figure 4d). The simulated data demonstrate these properties because the simulated background EEG contains activity in a range of frequency bands, but this activity is, by definition, randomly distributed across trials—there is no intertrial coherence of phase. The addition of a phasic peak imposes a dominant phase on the simulated single-trial EEG, because the peak occurs on every trial shortly after 0 ms. This addition therefore results in an uneven distribution of phase and significant intertrial phase coherence at all frequencies for which the phasic peak has significant spectral power (cf. Jervis et al., 1983). These results demonstrate that intertrial phase *coherence* is not unambiguous evidence of phase *resetting*: Observed biases in the distribution of phase might reflect the presence of a phasic signal rather than synchronization of ongoing EEG oscillations.

Analysis 2: Bandpass Filtered Data

Simple inspection of the raw data does not provide clear evidence of frontocentral theta oscillations: The peaks in the ERP waveform (Figure 3b) are somewhat irregularly spaced—being separated by 232 ms, 92 ms, and 116 ms—and the scalp topography of the Ne/ERN differs from the topography of the other peaks apparent in the waveform (Figure 3, lower panel). Nevertheless, it could be that oscillations generating the Ne/ERN are masked

by the presence of slow-wave activity. One analysis method used to deal with this masking problem is bandpass filtering, which aims to remove the effects of superimposed activity and thus uncover underlying oscillations (e.g., Luu & Tucker, 2001).

Apparently consistent with this rationale, when we 4–12 Hz bandpass filter our empirical data, the Ne/ERN appears to be part of a long-lasting theta oscillation. This oscillation is apparent both in the averaged ERP (Figure 5a) and in the phase-sorted EEG data (Figure 5b). Moreover, the oscillations apparent in the filtered data show a consistent frontocentral scalp topography (Figure 5, lower panel): Frontocentral negativities are observed at −148 ms, +52 ms, and +252 ms, occurring in alternation with frontocentral positivities at −48 ms and +152 ms. However, this pattern of results does not provide unambiguous evidence of synchronized oscillations, because corresponding patterns are observed in the simulated data: Oscillations are apparent in the filtered data—both in the simulated ERP (Figure 5c) and in the simulated single-trial EEG (Figure 5d)—and these oscillations are almost identical to those observed in the empirical data. Moreover, as shown in the lower panel of Figure 5, the oscillations in the filtered simulated data demonstrate a consistent frontocentral scalp topography.

The oscillations in the simulated data cannot reflect synchronization of ongoing EEG activity, because no such synchrony is present. Instead, the oscillations are a *ringing artifact* introduced by bandpass filtering. The origin of this artifact is illustrated in the right-hand panel of Figure 5. This panel shows a decomposition of the phasic peak into frequency components from 0 to 16 Hz, in which a common pattern is apparent: A central peak is flanked by a variable number of oscillations. When summed across all frequencies, the side oscillations cancel to leave a single central peak. Bandpass filtering amounts to removing contributions outside the frequencies of interest (gray lines), which results in a filtered signal that contains artifactual oscillations.[4] Because the magnitude of the ringing artifact will depend on the size of the

---

[4]A large ringing artifact is clear following bandpass filtering of the simulated ERP. Corresponding ringing artifacts are more difficult to discern in individual simulated EEG epochs (Figure 3d) because these artifacts are small ($< 10 \mu V$) relative to the amplitude of the background EEG ($> 50 \mu V$). Ringing artifacts are nevertheless present, as becomes apparent when many trials are averaged together so that activity in the background EEG averages out to roughly zero.
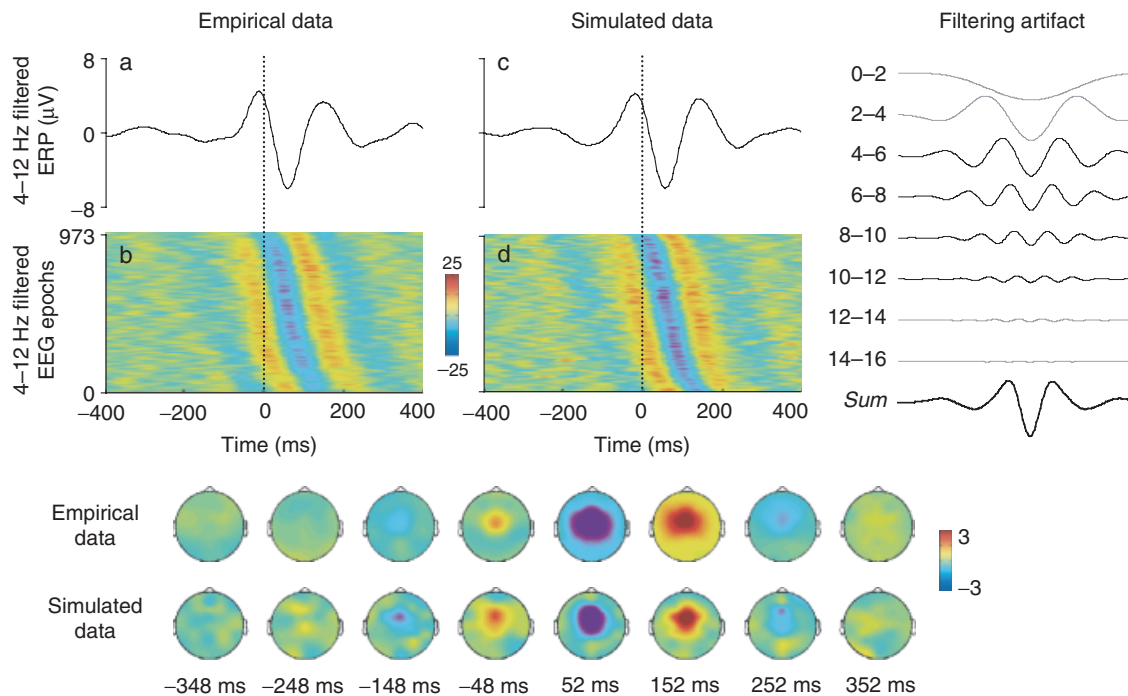
Figure 5. Bandpass filtering analysis. a: Empirical ERP waveform from electrode FCz, 4–12 Hz filtered. b: Single-trial empirical EEG epochs from electrode FCz, 4–12 Hz filtered and sorted according to phase at the theta frequency. c,d: Corresponding analyses of simulated data. Lower panel: Scalp topography of 4–12 Hz filtered empirical and simulated data between −348 ms and +352 ms. Upper right panel: Decomposition of the simulated Ne/ERN peak into frequency components from 0 to 16 Hz, and the sum of 4–12 Hz activity. The filtered waveform (thick line) contains artifactual oscillations around the central peak.

original peak, the size of the ringing artifact varies according to the topography of the original peak. For this reason, the simulated scalp topography of the oscillations created by the filtering artifact show a consistent frontocentral scalp topography (Figure 5, lower panel).

The ringing artifact is not the result of unusually sharp voltage transitions in the simulated peaks, nor is it caused by embedding the phasic peaks in background EEG noise that is oscillatory in nature: Figure 2b shows that the simulated data (black line) mimic very closely the transitions apparent in the empirical data (gray line), and Figure 5 (right panel) shows that the ringing artifact is apparent in data with no background noise. Instead, the results of the simulation demonstrate general difficulties that are faced when interpreting the results of bandpass filtering: Applying a narrow bandpass filter may filter out part of the signal itself, causing a distortion of this signal. The resulting ringing artifacts may create the appearance of oscillatory activity where none is present. Thus, the appearance of oscillations in bandpass filtered data is not unambiguous evidence of synchronized oscillations.

Analysis 3: ERP Amplitude and Spectral Power in the EEG

If ERPs are produced by synchronization of ongoing oscillations in the EEG, it follows that the amplitude of ERPs should depend upon the amplitude of these oscillations. Figure 6 (left panel) presents analysis results consistent with this prediction. Figure 6a shows single-trial EEG epochs for the 10% of trials with the highest theta power in the interval from − 180 ms to 320 ms relative to the response. Figure 6b shows a corresponding plot for the 10% of trials with the lowest theta energy in this time interval. Figure 6c shows the averaged ERPs for each trial subset. The Ne/

ERN is very clear in the trials with high theta power (red line), and entirely absent in trials with low theta activity (green line). Indeed, trials with high theta activity show some theta activity before and after the Ne/ERN peak; that is, there are large positive peaks, with power in the theta band, flanking the Ne/ERN. As shown in Figure 6d, trials with high theta activity are further marked by a much higher degree of intertrial phase coherence than trials with low theta power.

Once again, however, an analysis of the simulated data produces results very similar to those observed in the empirical data. As shown in the right panel of Figure 6, simulated trials with high theta activity are marked by a very large Ne/ERN that appears to be part of an ongoing oscillation (Figure 6g, red line). Correspondingly, intertrial phase coherence is high for this trial subset (Figure 6h, red line). In contrast, trials with low theta activity show little evidence of a simulated Ne/ERN peak (Figure 6g, green line) and have correspondingly little intertrial coherence of theta activity (Figure 6h, green line). The simulated data demonstrate these properties because the background EEG contains power at theta frequencies that may summate with or cancel out the phasic peak. Trials in which the signal peak summates with a peak in the noise are marked by high theta and a large phasic peak. Indeed, because the selected trials are those in which theta energy in the noise is almost perfectly in phase with the peak, the averaged ERP shows evidence of oscillations before and after the "true" peak. In contrast, trials in which the phasic peak is canceled out by fluctuations in the background EEG are marked by low theta power and almost no phasic peak. Therefore, a correlation between ERP amplitude and spectral power in the EEG does not provide unambiguous evidence that the ERP component is generated by synchronized oscillations: Similar patterns
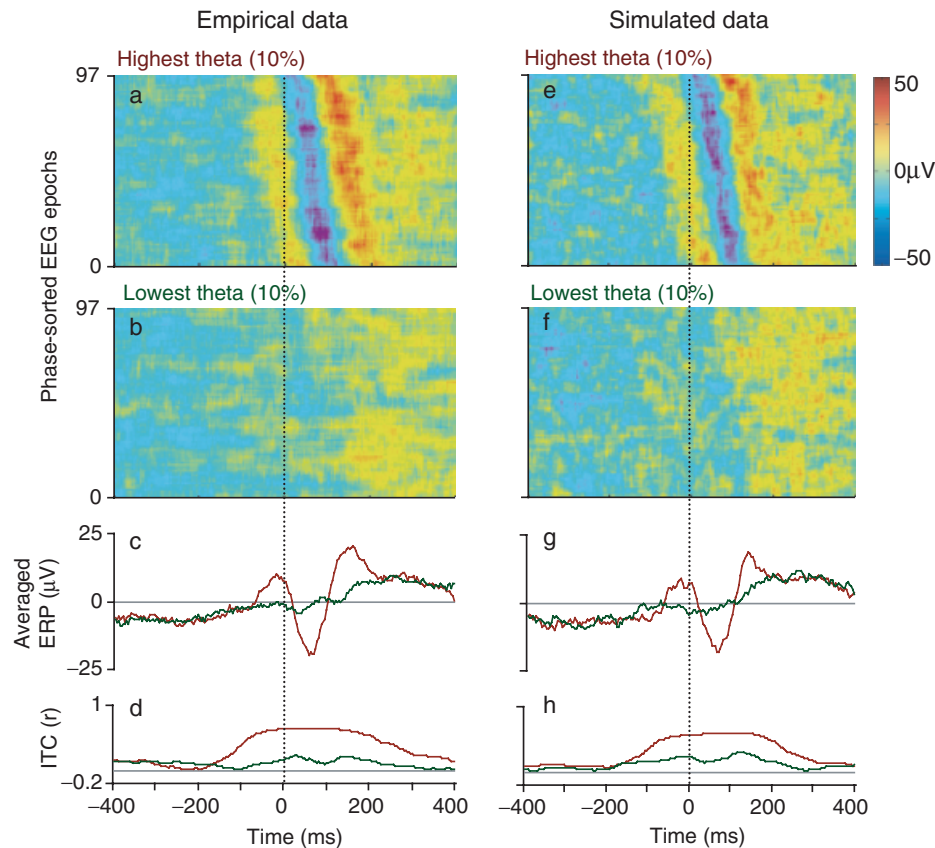
Figure 6. ERP in high- and low-power trial subsets. Single-trial EEG (a,b), averaged ERP (c), and intertrial coherence (ITC; d) for the empirical data at FCz, separating the 10% of trials with the highest theta energy (panel a and red curves) and the 10% of trials with the lowest theta energy (panel b and green curves). e–h: Corresponding analyses of the simulated data at FCz.

would be expected to occur when phasic activity summates or cancels with uncorrelated background EEG noise.

Analysis 4: Scalp Distribution of Spectral Power in the EEG and ERP

If ERPs are generated by synchronization of EEG oscillations, then ERP power at specific frequencies should be concentrated at scalp locations with the greatest power in the EEG at those frequencies. Figure 7 presents the relevant analysis for our empirical Ne/ERN data. The plots show the scalp distribution of relative power within four frequency bands—delta, theta, alpha, and beta—separately for the single-trial EEG and averaged ERP. A striking feature is that scalp locations with high ERP power have correspondingly high spectral power in the single-trial EEG data. Specifically, low-frequency (delta and theta) power is concentrated around midline central electrodes for both the single-trial EEG and averaged ERP.

The right-hand panel of Figure 7 presents a corresponding analysis of the simulated data. Replicating the pattern observed in the empirical data, the scalp topography of relative spectral power is very similar for the EEG and ERP data within each frequency band. Again, this property is largely restricted to low frequency delta and theta activity, both of which show a central midline focus. The explanation for this property is that the phasic components used in the simulation contain power in the low frequency bands: the slow-wave component contains delta band energy, the simulated Ne/ERN peak contains delta and theta energy. Because these phasic components contribute power both

to the single-trial EEG and to the averaged ERP, the topography of power in both will tend to reflect the (central midline) topography of the phasic ERP components. Thus, shared scalp distribution of spectral power in the ERP and EEG does not constitute unambiguous evidence of synchronized oscillations.

Analysis 5: Relative Spectral Power of the EEG and ERP

To the extent that the ERP contains greater power than expected by chance, one might infer that aspects of the EEG show event-related synchronization. We therefore calculated the spectral power of the averaged ERP and the power of the ERP that would be expected given a random distribution of phase across the 973 empirical EEG epochs. Figure 7 (bottom left panel) plots the resulting ratio of actual ERP power to the power expected assuming a random distribution of phase, separately for each of the 31 electrode locations, for frequencies from 2 to 20 Hz. The ratio expected assuming random phase is 1:1. The empirical data clearly deviate from this ratio in the delta and theta frequency bands. The scalp map shown illustrates that the deviation from random phase at 6 Hz is particularly large at midline frontocentral locations, consistent with the scalp topography of the Ne/ERN component. Evidently, these ERP data are characterized by event-related synchrony; that is, by nonrandom distribution of phase in the EEG.

However, as described above in the context of Analysis 1, phase coherence is not uniquely diagnostic of phase resetting. The present analysis provides further evidence of this point: As in the empirical data, the simulated data show much higher ERP
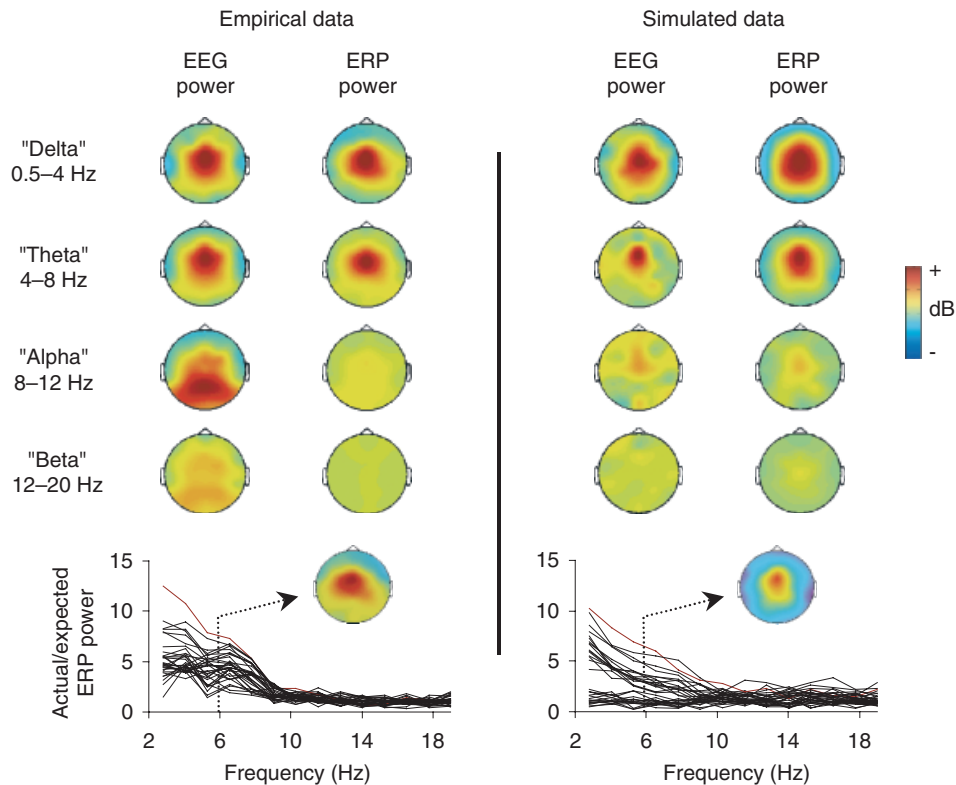
Figure 7. Scalp topography of power in the EEG and ERP. Upper left panel: Empirical scalp topography of relative EEG and ERP power in the delta, theta, alpha, and beta frequency bands. Lower left panel: Ratio of power in the averaged ERP compared with expected power assuming random distribution of phase in the single-trial EEG epochs across 31 electrodes (FCz in red). The scalp topography of the ratio of actual:expected ERP power is shown for 6-Hz activity. Upper and lower right panels: Corresponding analyses of the simulated data.

power than would be expected by chance, and particularly so at midline frontocentral scalp locations (Figure 7, bottom right panel). This pattern of results is not due to synchronization of oscillations, because no synchrony is present in the simulated data. Instead, the results follow from the fact that the contribution to the EEG from the fixed-latency phasic peak has power at a range of frequencies, and a phase (i.e., latency) that is consistent across epochs. Consequently, the phase of the EEG is unevenly distributed, and hence there is greater power in the ERP than would be expected by chance for all frequencies at which there is energy in the phasic peak. These results demonstrate that the observation of greater spectral power in the ERP than is expected by chance does not constitute unambiguous evidence that synchronized oscillations are present.

General Discussion

Our simulation results suggest that the analysis methods we have evaluated do not provide unambiguous evidence of phase synchronization of ongoing oscillations. The methods each make the assumption that the presence in the EEG of phase-coherent activity within a particular frequency band may be taken as evidence of event-related synchronization of oscillations. To the contrary, our simulations suggest—perhaps counterintuitively—that phasic bursts of neural activity may result in a similar type of phase-coherent oscillatory activity: The ''oscillations'' represent specific frequency components of the phasic activity,

and the ''phase-coherence'' is caused by consistent time-locking of the phasic activity to experimental events. In this way, event-related synchronization of oscillations and phasic bursts of neural activity may share many fundamental physical characterisics. It follows that these physical characteristics cannot be used as diagnostic markers of the presence of either kind of activity.

The most direct implication of our findings is that new analysis methods are required to distinguish between phasic activity and phase resetting, particularly in situations where there are increases in both power and intertrial phase coherence. Our simulation results suggest that in such situations there may not be clear, qualitative differences in activity generated by phasic neural events and by synchronization of ongoing oscillations. Instead, it may be necessary to focus on detailed, quantitative features of the data. For example, phasic bursts of activity typically contain energy at a range of spectral frequencies, whereas oscillatory activity can be restricted to a narrow frequency band. Conversely, whereas oscillatory activity may be temporally extended across multiple cycles of a particular frequency band, phasic activity is by definition temporally limited (notwithstanding the possibility of multiple successive phasic peaks; cf. Mangun, 1992). Thus, one potentially fruitful approach for future research will be to develop quantitative measures of the extent to which increases in power and phase coherence are spread in the time and frequency domains.

It may also prove useful to combine these new quantitative approaches with other methods that can be used to separate

activity from different neural sources, such as dipole modeling (e.g., Luu, Tucker, Derryberry, Reed, & Poulsen, 2003), Laplacian transformations (e.g., Vidal, Burle, Bonnet, Grapperon, & Hasbroucq, 2003), and spatial component analyses (e.g., ICA; Makeig, Westerfield, et al., 2002). The question addressed by these methods—of which neural sources contribute to observed EEG scalp distributions—is strictly orthogonal to the question of the nature of neural activity (phasic or oscillatory) within those sources. Nevertheless, spatial decomposition may be combined with analysis methods specifically aimed at distinguishing between phasic and oscillatory activity. The notion would be to preprocess the data to isolate activity in particular brain regions, then to subject this activity to rigorous, formal analyses to characterize the nature of activity within those brain regions.

In the context of new methods development, an important implication of the present research is that a useful approach to validating analysis methods is to apply them to simulated data sets. For example, extending the example above of new quantitative analysis methods, one might generate two data sets, one containing phasic events and the other synchronized oscillations. One could then compare the analysis results for these two data sets to establish the boundary conditions of variability in the time and frequency domains that distinguish between phasic and oscillatory activity. In this way, the new analysis methods could be rigorously evaluated against the known structure of the simulated data sets, before the methods are applied directly to empirical data (the structure of which can only be inferred).

Thus, the primary implication of the present research is methodological: Our findings suggest that the methods we have evaluated may not provide clear adjudication between the classical and synchronized oscillation theories of the origin of ERPs. Our findings do not challenge the general claim that rhythmic activity in the EEG contributes to ERPs. Indeed, there already exists evidence from other methods for the contribution of synchronized oscillations to the ERP (Klimesch et al., 2004; Makeig, Westerfield, et al., 2002; Rizzuto et al., 2003; Sayers et al., 1974), and there is increasing evidence for the importance of synchrony in ongoing oscillatory neural activity as a general organizing principle of the brain (Engel, Fries, & Singer, 2001; Salinas & Sejnowski, 2001; Varela, Lachaux, Rodriguez, & Martinerie, 2001; Ward, 2003; although see Shadlen & Movshon, 1999 for a dissenting voice). In this context, an important avenue for future research will be to investigate the extent to which observations of synchronous activity between brain regions (e.g., Klopp, Marinkovic, Chauvel, Nenov, & Halgren, 2000; Mima, Oluwatimilehin, Hiraoka, & Hallet, 2001; Rodriguez et al., 1999) are due to coincident bursts of phasic neural activity versus between-region synchronization of ongoing oscillatory activity.

Finally, we note that our simulation results do not prove that the Ne/ERN reflects a transient burst of neural activity rather than synchronized theta oscillations. Nor do our simulations bear on the ongoing debate between competing functional theories of the Ne/ERN in terms of error detection (Falkenstein et al., 1990; Gehring et al., 1993), reinforcement learning (Holroyd & Coles, 2002), action regulation (Luu et al., 2003), or response conflict monitoring (Yeung et al., in press). Indeed, it remains an open question whether the nature of underlying neural activity will have significant impact on this theoretical debate. For example, the conflict monitoring theory proposes that the Ne/ERN reflects the detection of response conflict in the period after incorrect responses (Yeung et al., in press), but does not specify whether detection of conflict leads to phase resetting of ongoing theta oscillations or phasic bursts of activity. In either case, variability in the degree of conflict across experimental conditions would be reflected in variability in the amplitude of the Ne/ERN—exactly the prediction made by the existing theory (Yeung et al., in press). Similarly, the reinforcement learning theory—which holds that the Ne/ERN is associated with a phasic reduction in dopamine (Holroyd & Coles, 2002)—is agnostic on whether this dopamine reduction causes a phasic burst of neural activity or phase resetting of EEG theta rhythms in medial frontal regions (e.g., Luu & Tucker, 2002). Thus, an issue to be considered in future research is the extent to which debates about the neural basis (phasic or oscillatory) of particular ERP components should influence theoretical debates about the functional basis of those components.

REFERENCES

Başar, E. (1980). *EEG brain dynamics: Relation between EEG and brain evoked potentials.* Amsterdam: Elsevier.

Başar, E., Başar-Eroglu, C., Parnefjord, R., Rahn, E., & Schürmann, M. (1992). Evoked potentials: Ensembles of brain induced rhythmicities in the alpha, theta and gamma ranges. In E. Başar & T. H. Bullock (Eds.), *Induced rhythms in the brain* (pp. 155–181). Boston, MA: Birkhauser.

Coles, M. G. H., Gratton, G., & Fabiani, M. (1990). Event-related brain potentials. In J. T. Cacioppo & L. G. Tassinary (Eds.), *Principles of psychophysiology: Physical, social and inferential elements* (pp. 413–455). Cambridge, UK: Cambridge University Press.

Coles, M. G. H., & Rugg, M. D. (1995). Event-related brain potentials: An introduction. In M. D. Rugg & M. G. H. Coles (Eds.), *Electrophysiology of mind: Event-related brain potentials and cognition* (pp. 1–26). Oxford: Oxford University Press.

Demiralp, T., Ademoglu, A., Schürmann, M., Başar-Eroglu, C., & Başar, E. (1999). Detection of P300 waves in single trials by the Wavelet Transform (WT). *Brain and Language, 66,* 108–128.

Domino, E. F., Matsuoka, S., Waltz, J., & Cooper, I. (1964). Simultaneous recordings of scalp and epidural somatosensory-evoked responses in man. *Science, 145,* 1199–1200.

Engel, A. K., Fries, P., & Singer, W. (2001). Dynamic predictions: oscillations and synchrony in top-down processing. *Nature Reviews Neuroscience, 2,* 704–716.

Eriksen, B. A., & Eriksen, C. W. (1974). Effects of noise letters upon the identification of target letters in a non-search task. *Perception and Psychophysics, 16,* 143–149.

Falkenstein, M., Hohnsbein, J., & Hoorman, J. (1995). Event-related potential correlates of errors in reaction tasks. In G. Karmos, M. Molnar, V. Csepe, I. Czigler, & J. E. Desmedt (Eds.), *Perspectives of event-related potentials research* (pp. 287–296). Amsterdam: Elsevier.

Falkenstein, M., Hohnsbein, J., Hoorman, J., & Blanke, L. (1990). Effects of errors in choice reaction tasks on the ERP under focused and divided attention. In C. H. M. Brunia, A. W. K. Gaillard, & A. Kok (Eds.), *Psychophysiological brain research* (Vol. 1, pp. 192–195). Tilburg, the Netherlands: Tilburg University Press.

Gehring, W. J., Goss, B., Coles, M. G. H., Meyer, D. E., & Donchin, E. (1993). A neural system for error detection and compensation. *Psychological Science, 4,* 385–390.

Gevins, A., Smith, M. E., McEvoy, L. K., & Yu, D. (1997). High-resolution EEG mapping of cortical activation related to working memory: Effects of task difficulty, type of processing, and practice. *Cerebral Cortex, 7,* 374–385.

Goff, W. R., Allison, T., & Vaughan, H. G. (1978) The functional neuroanatomy of event related potentials. In E. Callaway, P. Tueting, & S. Koslow (Eds.), *Event-related brain potentials in man* (pp. 1–91). New York: Academic Press.

Holroyd, C. B., & Coles, M. G. H. (2002). The neural basis of human error processing: Reinforcement learning, dopamine, and the error-related negativity. *Psychological Review*, *109*, 679–709.

Jansen, B. H., Agarwal, G., Hegde, A., & Boutros, N. N. (2003). Phase synchronization of the ongoing EEG and auditory EP generation. *Clinical Neurophysiology*, *114*, 79–85.

Jervis, B. W., Nichols, M. J., Johnson, T. E., Allen, E., & Hudson, N. R. (1983). A fundamental investigation of the composition of auditory evoked potentials. *IEEE Transactions on Biomedical Engineering*, *30*, 43–50.

Kahana, M. J., Sekuler, R., Caplan, J. B., Kirschen, M., & Madsen, J. R. (1999). Human theta oscillations exhibit task dependence during virtual maze navigation. *Nature*, *399*, 781–784.

Karakaş, S., Erzengin, Ö. U., & Başar, E. (2000). The genesis of human event-related responses explained through the theory of oscillatory neural assemblies. *Neuroscience Letters*, *285*, 45–48.

Klimesch, W. (1999). EEG alpha and theta oscillations reflect cognitive and memory performance: A review and analysis. *Brain Research Reviews*, *29*, 169–195.

Klimesch, W., Schack, B., Schabus, M., Doppelmayr, M., Gruber, W., & Sauseng, P. (2004). Phase-locked alpha and theta oscillations generate the P1–N1 complex and are related to memory performance. *Cognitive Brain Research*, *19*, 302–316.

Klopp, J., Marinkovic, K., Chauvel, P., Nenov, V., & Halgren, E. (2000). Early widespread cortical distribution of coherent fusiform face selective activity. *Human Brain Mapping*, *11*, 286–293.

Luu, P., & Tucker, D. M. (2001). Regulating action: Alternating activation of midline frontal and motor cortical networks. *Clinical Neurophysiology*, *112*, 1295–1306.

Luu, P., & Tucker, D. M. (2002). Self-regulation and the executive functions: Electrophysiological clues. In A. Zani & A. M. Proverbio (Eds.), *The cognitive electrophysiology of mind and brain* (pp. 199–223). San Diego, CA: Academic Press.

Luu, P., Tucker, D. M., Derryberry, D., Reed, M., & Poulsen, C. (2003). Electrophysiologic responses to errors and feedback in the process of action regulation. *Psychological Science*, *14*, 47–53.

Makeig, S., Luu, P., & Tucker, D. M. (2002, June). Do 'brainstorms' help turn intentions into actions? Paper presented at the 8th international conference on functional mapping of the human brain, Sendai, Japan.

Makeig, S., Westerfield, M., Jung, T.-P., Enghoff, S., Townsend, J., Courchesne, E., & Sejnowski, T. J. (2002). Dynamic brain sources of visual evoked responses. *Science*, *295*, 690–694.

Mangun, G. R. (1992). Human visual evoked potentials: Induced rhythms or separable components? In E. Başar & T. H. Bullock (Eds.), *Induced rhythms in the brain* (pp. 217–231). Boston, MA: Birkhauser.

Mima, T., Oluwatimilehin, T., Hiraoka, T., & Hallett, M. (2001). Transient interhemispheric neuronal synchrony correlates with object recognition. *Journal of Neuroscience*, *21*, 3942–3948.

Penny, W. D., Kiebel, S. J., Kilner, J. M., & Rugg, M. D. (2002). Event-related brain dynamics. *Trends in Neurosciences*, *25*, 387–389.

Pfurtscheller, G., & Lopes da Silva, F. H. (1999). Event-related EEG/MEG synchronization and desynchronization: Basic principles. *Clinical Neurophysiology*, *110*, 1842–1857.

Rizzuto, D. S., Madsen, J. R., Bromfield, E. B., Schulze-Bonhage, A., Seelig, D., Aschenbrenner-Scheibe, R., & Kahana, M. J. (2003). Reset of human neocortical oscillations during a working memory task. *Proceedings of the National Academy of Sciences, USA*, *100*, 7931–7936.

Rodriguez, E., George, N., Lachaux, J.-P., Martinerie, J., Renault, B., & Varela, F. (1999). Perception's shadow: Long-distance synchronization of human brain activity. *Nature*, *397*, 430–433.

Salinas, E., & Sejnowski, T. J. (2001). Correlated neuronal activity and the flow of neural information. *Nature Reviews Neuroscience*, *2*, 539–550.

Sayers, B. M., Beagley, H. A., & Henshall, W. R. (1974). The mechanism of auditory evoked EEG responses. *Nature*, *247*, 481–483.

Shadlen, M. N., & Movshon, J. A. (1999). Synchrony unbound: A critical evaluation of the temporal binding hypothesis. *Neuron*, *24*, 67–77.

Shah, A. S., Bressler, S. L., Knuth, K. H., Ding, M., Mehta, A. D., Ulbert, I., & Schroeder, C. E. (2004). Neural dynamics and the fundamental mechanisms of event-related brain potentials. *Cerebral Cortex*, *14*, 476–483.

Tallon-Baudry, C., & Bertrand, O. (1999). Oscillatory gamma activity in humans and its role in object representation. *Trends in Cognitive Sciences*, *3*, 151–162.

Tallon-Baudry, C., Bertrand, O., Delpuech, C., & Pernier, J. (1996). Stimulus specificity of phase-locked and non-phase-locked 40 Hz visual responses in human. *Journal of Neuroscience*, *16*, 4240–4249.

Varela, F., Lachaux, J.-P., Rodriguez, E., & Martinerie, J. (2001). The brainweb: Phase synchronization and large-scale integration. *Nature Reviews Neuroscience*, *2*, 229–239.

Vaughan, H. G. (1969). The relationship of brain activity to scalp recordings of event-related potentials. In E. Donchin & D. B. Lindsley (Eds.), *Average evoked potentials: Methods, results, and evaluations*. Washington DC: U.S. Government Printing Office.

Vidal, F., Burle, B., Bonnet, M., Grapperon, J., & Hasbroucq, T. (2003). Error negativity on correct trials: A reexamination of available data. *Biological Psychology*, *64*, 265–282.

Ward, L. M. (2003). Synchronous neural oscillations and cognitive processes. *Trends in Cognitive Sciences*, *7*, 553–559.

Weinberg, H. (1978). Comments on methods of signal analysis and signal detection. In D. Otto (Ed.), *Multidisciplinary perspectives on event-related potential research*. Washington DC: U.S. Government Printing Office.

Yeung, N., Botvinick, M. M., & Cohen, J. D. (in press). The neural basis of error detection: Conflict monitoring and the error-related negativity. *Psychological Review*, *111*.